Progress In Electromagnetics Research Letters, Vol. 55, 145–151, 2015

A 60 GHz End-Fire High-Gain Tapered Slot Antenna with Side-Lobe Suppression

Ning Wang and Peng Gao*

Abstract—A simple end-fire high-gain antenna with side-lobe level suppression is proposed for 60 GHz technology in this paper. The antenna has a tapered slot radiation patch which is obtained by subtracting a quarter of ellipse from a bigger quarter. Two reflecting circle units (RCU) are located at both sides of radiant patch to suppress side-lobe level of radiation patterns. The antenna has a simple two-layered planar structure with on via and is fabricated on a Rogers 4350 substrate with a compact size of 15 mm × 15 mm. Simulated and measured results match well, and both show its good characteristics of impedance matching, stable radiation patterns and steady peak gains above 10 dBi across 57–64 GHz, which makes it fit 60 GHz wireless communication systems.

1. INTRODUCTION

With the rapid development of wireless technology, an unlicensed frequency band of 7 GHz centered at 60 GHz has become an interesting and potential candidate for the next generation (5G) wireless personal area network (WPAN) [1–4]. According to IEEE 802.15.3c, it provides mandatory data rates exceeding 1 Gb/s and can be used for applications as uncompressed video streaming, high data wireless transferring, mobile distributed computing, etc. [4]. However, 60 GHz is at the limit of atmospheric absorption [5], and high antennas are valuable to be researched on to enable a longer way communications. In the past decade, there have been a lot of reports on 60 GHz high-gain antennas [6–13]. In [7], Waleed et al. proposed a multi-layer antenna using mounted horn integrated on FR4, which realize a gain up to 11.65 dBi. In [8], Li and Luk demonstrate a substrate integrated waveguide (SIW)-fed patch antenna array and a gain 19.6 dBi is achieved. Using LTCC technology, a Yagi antenna presented in [9] achieves a peak gain of 6 dBi and a 4 × 4 array of Yagi antenna in [10] reaches max gain of 18 dBi. However, these antennas either are multi-layered or have complex structures, which possibly bring difficulties to fabrications and cost-reduction. Recently, a planar fan-like antenna was presented [13]. With a peak gain of 7.6 dBi, it has been the highest for a simple designed planar 60 GHz antenna reported so far and still has space to improve.

In this paper, a simple planar tapered slot antenna basing on substrate Rogers 4350 is proposed. This antenna has two blade-like antipodal tapered slot patches which are crossed symmetrically on both sides of the substrate. Then in order to obtain a lower side-lobe level, tow circle patches are located two sides of the radiant patch and side-lobe level is suppressed by 5 dB. Details of antenna design, simulation and measurement are presented below.

2. ANTENNA DESIGN

The geometry of the proposed antenna is shown in Figure 1(a), which contains four parts including a 50-Ω microstrip feeding line, a tapered parallel plate waveguide, a tapered radiant patch and reflecting circle

Received 7 July 2015, Accepted 14 August 2015, Scheduled 30 August 2015
* Corresponding author: Peng Gao (penggao@uestc.edu.cn).
The authors are with the Research Institute of Electronic Science and Technology, University of Electronic Science and Technology of China, Chengdu 611731, China.

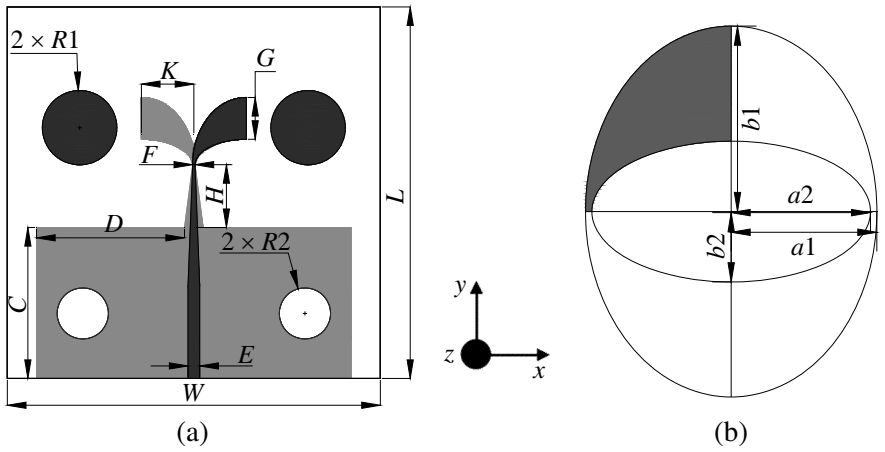

Figure 1. Geometry of the proposed antenna: (a) Total geometry; (b) fabrication of radiant patch.

units. The radius of circle holes near the microstrip feeding line is $R2 = 1.1$ mm. The total dimension of the proposed antenna is 15 mm × 15 mm, which is fabricated on a Rogers 4350 substrate with a relative permittivity of 3.66, dielectric loss tangent of 0.004 and thickness of 0.254 mm. The blade-like tapered slot radiant patch is obtained by subtracting a quarter of ellipse from a bigger quarter, as shown in Figure 1(b). The dimensions of the bigger ellipse are: $a1 = 2.3$ mm, $b1 = 2.9$ mm while the smaller ones are: $a2 = 2.2$ mm, $b2 = 1.1$ mm. In order to obtain the low side-lobe level, two reflecting circle units are located at both sides of the radiant patch, where the radius of the circle units is $R1 = 1.6$ mm. The rest dimensions in Figure 1(a) are: $E = 0.5$ mm, $W = 16$ mm, $L = 16$ mm, $C = 6.5$ mm, $D = 6.35$ mm, $H = 2.7$ mm, $F = 0.1$ mm, $G = 1.8$ mm, $K = 2.25$ mm.

2.1. Reflecting Circle Unit Design

The structure of Reflecting Circle Units (RCUs) is shown in Figure 2(a), while Figure 2(b) is their simulated frequency response by using Ansys HFSS V13. It is mentioned that ZY-plane and ZX-plane are separately assigned perfect magnetic conducting (PMC) and perfect electric conducting (PEC) boundary. XY-planes in positive Z direction and negative Z direction are separately assigned with wave port 1 and 2. As depicted in Figure 2(b), return losses (S_{11}) are less than 0.06 dB and insertion losses (S_{21}) are bigger than 15 dB across 57–64 GHz, which both denote that most energy has been reflected

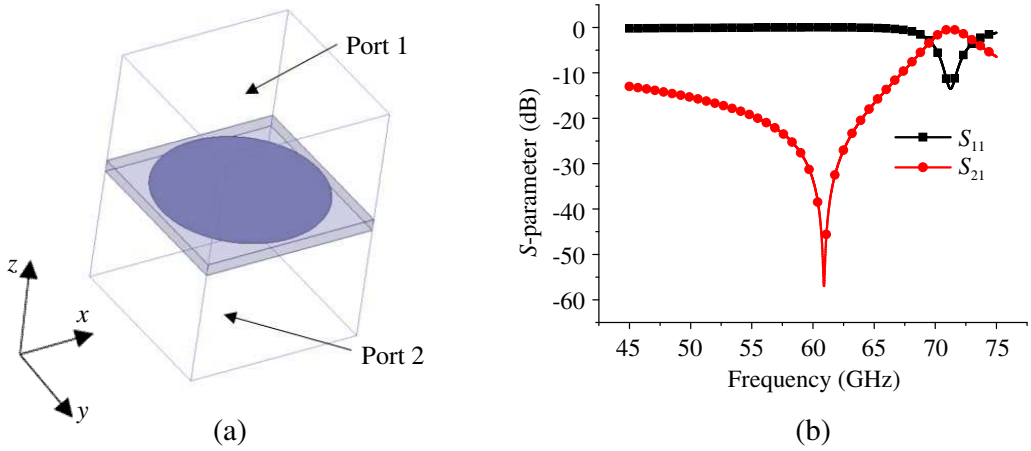

Figure 2. Reflecting circle unit: (a) Structure; (b) band-stop characteristics of S-parameters.

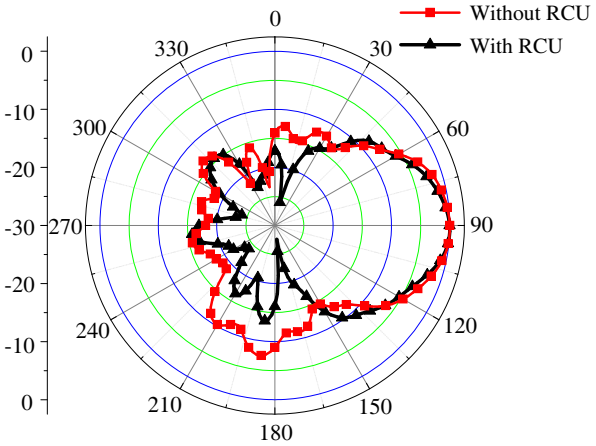

Figure 3. The normalized radiation patterns of the proposed antenna with and without RCUs in the XY-plane at 60 GHz.

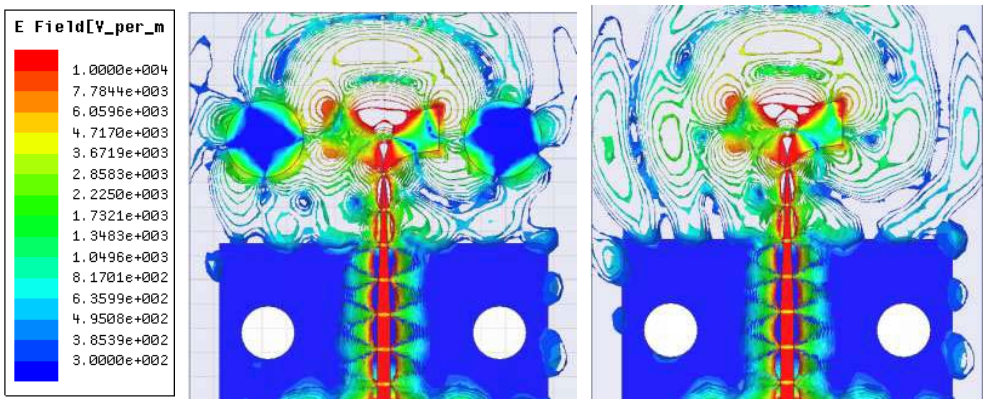

(a) (b)

Figure 4. E-Field distribution of antenna (a) with RCU and (b) without RCU at 60 GHz.

and little power flux pass through the RCUs, namely they have perfect band-stop characteristics. In this case, by locating the RCUs at both sides of the radiant patch, electromagnetic wave transmitting to positive X direction or negative X direction is successfully blocked, which let the side-lobe level of XY-plane radiation pattern reduced at least 5 dB, as shown in Figure 3. The comparison between E-Field distribution with and without RCUs is shown in Figure 4. It is obvious that the E-Field intensity is reduced greatly at both sides of radiant patch when RCUs are located.

2.2. Antenna Measurement System

Figure 5 shows the measurement system sketch for radiating properties. Figure 6 is a photo of the system in lab. In the measuring process, a vector network analyzer (VNA) Agilent PNA-X N5247A is connected the device under test (DUT) as a transmitter, and a high sensitive spectrum analyzer (SA) is used to connect to a standard horn as a receiver. The horn antenna is put on a nylon slide rail, which runs forth and back. The gains of the proposed antenna are calculated using the following equation.

$$G_t\,(\text{dB}) = P_r\,(\text{dBm}) - P_t\,(\text{dBm}) - G_r\,(\text{dB}) + L_r\,(\text{dB}) + L_t\,(\text{dB}) + L_s\,(\text{dB}) \tag{1}$$

In Equation (1), G_t is the gain of DUT and G_r the gain of standard horn. P_t and P_r are the transmitting and receiving power of VNA and SA separately. L_t and L_r are the losses of cables and connectors in

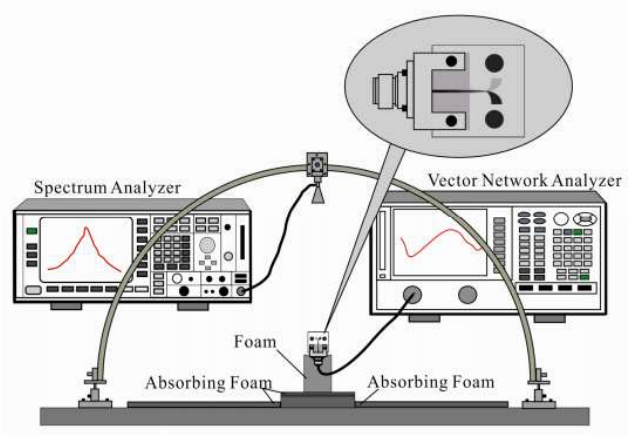

Figure 5. Sketch of the antenna measurement system.

Figure 6. Photograph of the antenna measurement system in lab.

the transmitter and receiver, respectively. L_s is the loss in free space, which is calculated as

$$L_s = 20\log_{10}\frac{4\pi R}{\lambda}. \tag{2}$$

In Equation (2), R is distance between receiving and transmitting antenna and λ is the wavelength of free space.

3. EXPERIMENTAL RESULTS AND DISCUSSION

3.1. Fabrication and Measurements

The antenna is fabricated as shown in Figure 7, and a 1.85 mm end-launch connector is connected to the microstrip line for measuring. Simulated and measured return losses are compared in Figure 8. It is found that simulated and measured results match well, and this antenna has good impedance match with return loss less than -10 dB across 52–65 GHz.

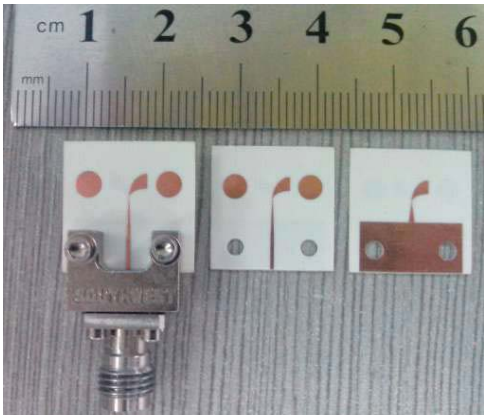

Figure 7. Photograph of fabrication.

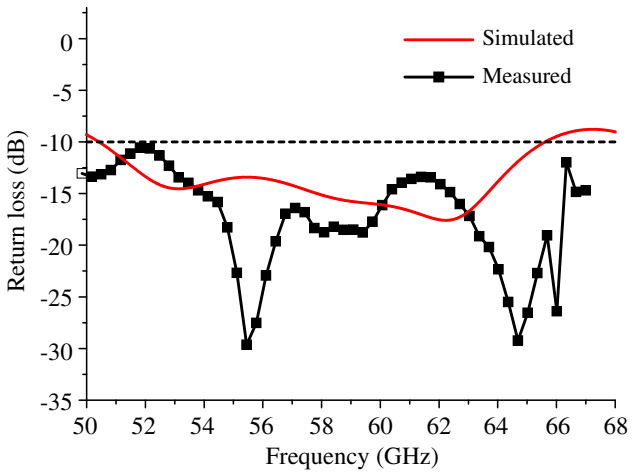

Figure 8. Comparisons of simulated and measured return loss of the proposed antenna.

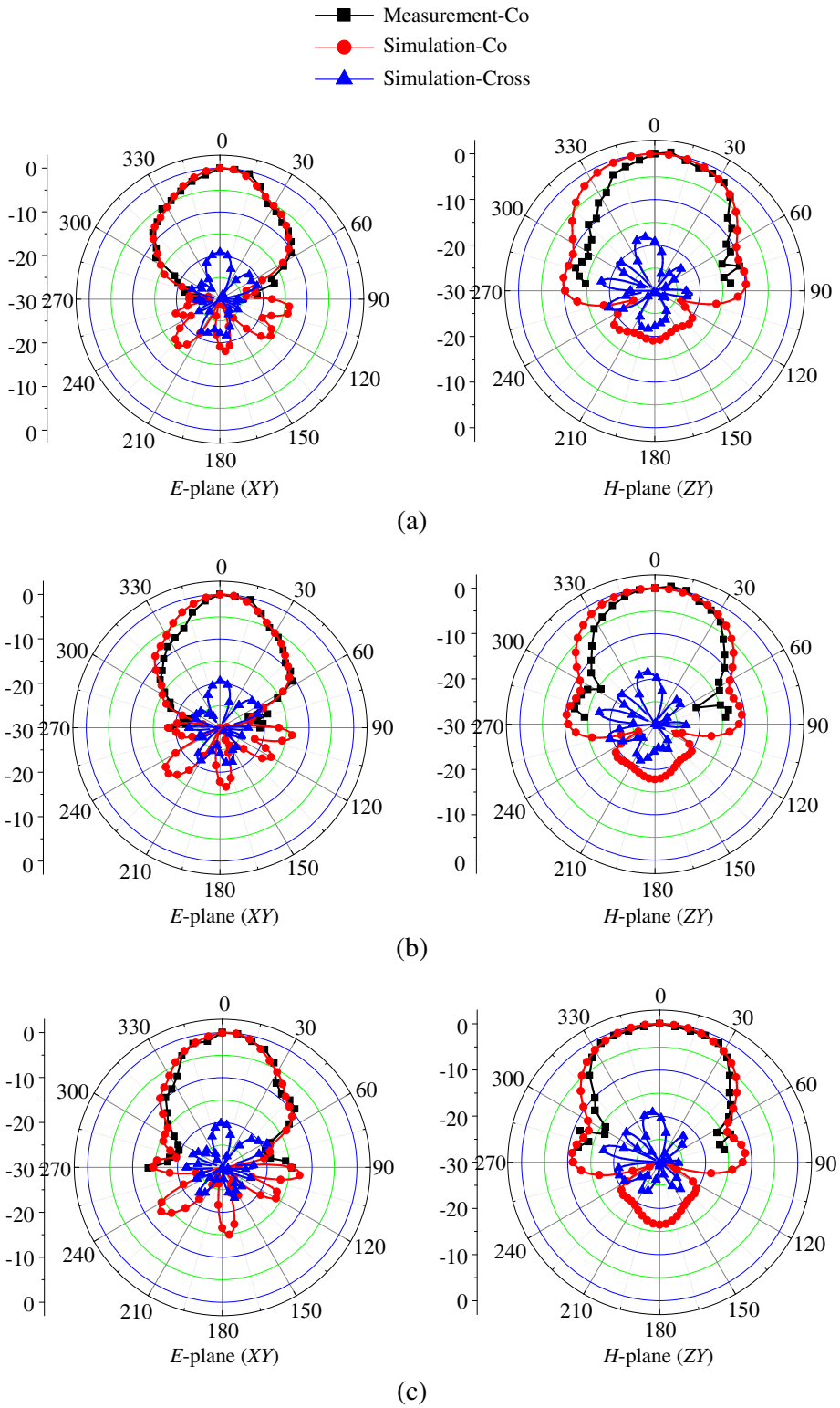

Figure 9. Simulated and measured radiation pattern of the proposed antenna at (a) 58 GHz, (b) 60 GHz, (c) 62 GHz.

Table 1. Simulated and measured peak gains of the proposed antenna.

Frequency (GHz)	Simulated peak gain (dBi)	Measured peak gain (dBi)
58	9.6	10.1
60	10	10.4
62	10.2	10.5
64	10.1	10.2

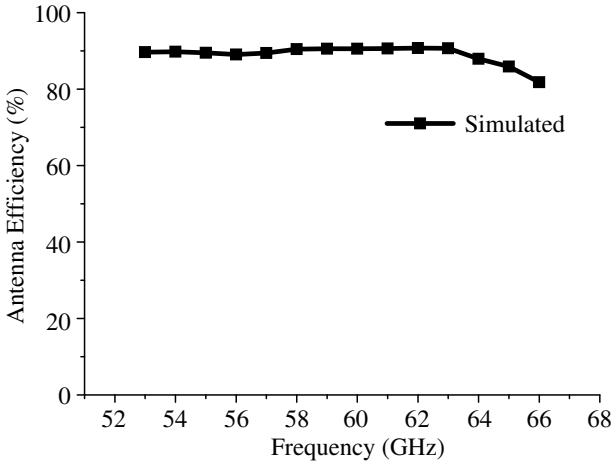

Figure 10. Simulated efficiency of the proposed antenna.

3.2. Radiation Performance

The E-plane (XY-plane) and H-plane (ZY-plane) co-polarisation radiation patterns are simulated and measured at three frequencies 58 GHz, 60 GHz and 62 GHz as shown in Figure 9. And the simulated and measured results match well and exhibit good stable radiation and low side-lobe level across 57–64 GHz. Simulated cross-polarisation radiation patterns are also given to show good radiant properties of the proposed antenna. Simulated and measured peak gains are shown in Table 1. The peak gains are above 10 dBi with various less than 1 dB and the discrepancy between simulation and measurement is about 0.4 dB. The antenna also has a high efficiency nearly 90% shown in Figure 10.

4. CONCLUSION

In this paper, a 60 GHz planar end-fire high-gain antenna is designed, analyzed and measured. It has a simple two-layered structure with no via, which is easy to fabricate and be integrated with traditional PCB. This antenna has a dimension of 15 mm × 15 mm and is fabricated by using a Rogers 4350 substrate with a thickness of 0.254 mm and relative permittivity of 3.66. Simulated and measured results match well, and both show the antenna's good characteristics of return losses less than −10 dB, favorable radiation pattern, stable high gains above 10 dBi with various less than 1 dB across 57–64 GHz. Therefore, it is suitable for 60 GHz wireless communication systems.

REFERENCES

1. Cabric, D., M. S. W. Chen, D. A. Sobel, and J. Yang, "Future wireless systems UWB, 60 GHz and cognitive radios," *IEEE Custom Integrated Circuits Conference*, 793–796, 2005.

2. Zhang, Y. P. and D. Liu, "Antenna-on-chip and antenna-in-package solutions to highly integrated millimeter-wave devices for wireless communications," *IEEE Trans. on Antennas and Propagat.*, Vol. 57, No. 10, 2009.
3. Andrews, J. G., S. Buzzi, W. Choi, S. V. Hanly, A. Lozano, A. C. K. Soong, and J. C. Zhang, "What will 5G be?" *IEEE Joural on Selected Areas in Communications*, Vol. 32, No. 6, 1065–1082, 2014.
4. Baykas, T., C.-S. Sum, L. Zhou, J. Wang, M. A. Rahman, H. Harada, and S. Kato, "IEEE 802.15.3c: The first IEEE wireless standard for data rates over 1 Gb/s," *IEEE Commun. Mag.*, Vol. 49, No. 7, 114–121, 2011.
5. Pietraski, P., D. Britz, A. Roy, R. Pragada, and G. Charlton, "Millimeter wave and terahertz communications: Feasibility and challenges," *ZTE Communications*, Vol. 10, No. 4, 2012.
6. Alhalabi, R. A., Y.-C. Chiou, and G. M. Rebeiz, "Self-shielded high-efficiency Yagi-Uda antennas for 60 GHz communications," *IEEE Trans. on Antennas and Propagat.*, Vol. 59, No. 3, 742–750, 2011.
7. Sethi, W. T., H. Vettikalladi, B. K. Minhas, and M. A. Alkanhal, "High gain and wide-band aperture-coupled microstrip patch antenna with mounted horn integrated on FR4 for 60 GHz communication systems," *IEEE Symposium on Wireless Technology and Applications (ISWTA)*, 359–362, 2013.
8. Li, Y. and K.-M. Luk, "Low-cost high-gain and broadband substrate integrated-waveguide-fed patch antenna array for 60-GHz band," *IEEE Trans. on Antennas and Propagat.*, Vol. 62, No. 11, 2014.
9. Kramer, O., T. Djerafi, and K. Wu, "Very small footprint 60 GHz stacked Yagi antenna array," *IEEE Trans. on Antennas and Propagat.*, Vol. 59, No. 9, 3204–3210, 2011.
10. Sun, M., Y. P. Zhang, K. M. Chua, L. L. Wai, D. Liu, and B. P. Gauche, "Integration of Yagi antenna in LTCC package for differential 60-GHz radio," *IEEE Trans. on Antennas and Propagat.*, Vol. 56, No. 8, 2008.
11. Dadgarpour, A., B. Zarghooni, B. S. Virdee, and T. A. Denidni, "Millimeter-wave high-gain end-fire bow-tie antenna," *IEEE Trans. on Antennas and Propagat.*, Vol. 63, No. 5, 2337–2342, 2015.
12. Cabrol, P. and P. Pietraski, "60 GHz patch antenna array on low cost liquid crystal polymer (LCP) substrate," *IEEE Systems, Applications and Technology Conference (LISAT)*, 1–6, 2014.
13. Sun, M., X. Qing, and Z. N. Chen, "60-GHz end-fire Fan-like antennas with wide beamwidth," *IEEE Trans. on Antennas and Propagat.*, Vol. 61, No. 4, 1616–1622, 2013.